2668 Vol. 40, No. 11 / June 1 2015 / Optics Letters Letter

Optics Letters

High-power mid-infrared high repetition-rate supercontinuum source based on a chalcogenide step-index fiber

STEFAN KEDENBURG,* TOBIAS STEINLE, FLORIAN MÖRZ, ANDY STEINMANN, AND HARALD GIESSEN

4th Physics Institute and Research Center SCOPE, University of Stuttgart, 70550 Stuttgart, Germany
*Corresponding author: s.kedenburg@pi4.uni-stuttgart.de

Received 30 March 2015; revised 15 May 2015; accepted 18 May 2015; posted 19 May 2015 (Doc. ID 236877); published 1 June 2015

We demonstrate a tunable and robust femtosecond supercontinuum source with a maximum output power of 550 mW and a maximum spectral width of up to 2.0 μm, which can cover the mid-infrared region from 2.3 μm up to 4.9 μm by tuning the pump wavelength. As_2S_3 chalcogenide step-index fibers with core diameters of 7 and 9 μm are pumped at different wavelengths from 2.5 μm up to 4.1 μm with femtosecond pulses by means of a post-amplified optical parametric oscillator pumped by an Yb:KGW laser. The spectral behavior of the supercontinuum is investigated by changing the pump wavelength, core diameter, fiber length, and pump power. Self-phase modulation is identified as the main broadening mechanism in the normal dispersion regime. This source promises to be an excellent laboratory tool for infrared spectroscopy owing to its high brilliance as demonstrated for the CS_2-absorption bands around 3.5 μm.

OCIS codes: (060.4370) Nonlinear optics, fibers; (160.4330) Nonlinear optical materials; (320.6629) Supercontinuum generation.

http://dx.doi.org/10.1364/OL.40.002668

Fiber-based supercontinuum sources benefit from their good beam quality and divergence that are needed for spectroscopy and metrology as well as defense applications. Their spatial coherence, broad bandwidth, and high brightness overcome the current limitations of mid-infrared sources, such as thermal emitters or synchrotron radiation. Particularly, supercontinuum generation in the mid-infrared based on chalcogenide fibers (chalcogen elements S, Se) have represented an area of intense research [1] due to their wide transmission range [2] and strong nonlinear refractive index n_2 (100 times larger compared to fused silica) [3].

Several demonstrations have been based on suspended-core chalcogenide fibers [4–6] with small core sizes to increase the nonlinearity and to down-shift the zero dispersion wavelength (ZDW). By pumping an As_2S_3 fiber in the anomalous dispersion region, the spectral range is rather broadband from 0.7 μm up to 3.8 μm [4] due to the contribution of soliton dynamics. However, the sources have been limited in flatness of the spectra, robustness, as well as average power (<30 mW) [4].

Step-index fiber-based supercontinuum laser systems possess the advantage of higher optical damage threshold and environmental stability (e.g., being nonhydroscopic). Hudson *et al.* [7] have used a kHz optical parametric chirped-pulse amplifier to pump a 9-μm-diameter As_2S_3 step-index fiber and have obtained a spectrum that spanned from 1.6 to 5.9 μm with an average power that was limited to 8 mW. With a 16-μm-diameter As_2Se_3 high-NA step-index fiber, a supercontinuum covering 1.4–13.3 μm region has been generated with limited average power in the μW level [8]. In the work of Gattass *et al.* [9], a 2-m-long 10-μm-diameter As_2S_3 step-index fiber pumped at a central wavelength of 2.45 μm with a spectral bandwidth of 100 nm from a highly nonlinear fiber has been used. The achieved emission covered the wavelength range from 1.9 to 4.8 μm with an output power of 565 mW at a repetition rate of 10 MHz. Xie *et al.* [10] developed a step-index fiber tapered at both ends that combined the properties of step-index and suspended-core fibers. In a Ge-As-Se waveguide [11] and step-index fiber [12], the group of Yu *et al.* have generated broad supercontinua in the mid-IR up to a wavelength of 10 μm with an average output power of 1.26 mW at a repetition rate of 21 MHz. Owing to the geometric design and the long-pump wavelength of around 4 μm, Yu *et al.* were able to pump close to the ZDW, and the spectral broadening was dominated by anomalous dispersion effects.

A different intriguing approach developed by Jiang *et al.* [13] has been based on a solid-core ZBLAN photonic crystal fiber enabling the extension of the supercontinuum down into the deep ultraviolet wavelength region. In a step-index ZBLAN fiber, a high-power mid-infrared supercontinuum could be generated with an output power of up to 13 W and a spectral coverage from 1.9 to 4.3 μm [14]. In a further interesting work with a tellurite fiber [15], it has been possible to shift the ZDW down to 2 μm by maintaining a robust W-type index profile fiber geometry. The achieved supercontinuum in a 1-m-long tellurite fiber pumped near the ZDW with 26 ps pulses spanned from 1.25 to 4.50 μm.

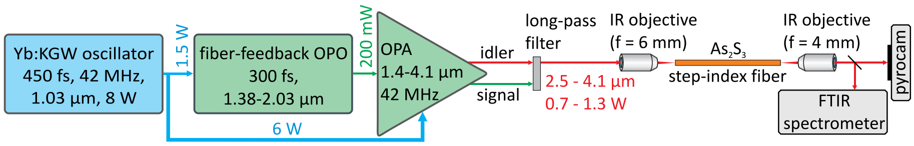

Fig. 1. Schematic of the experimental setup consisting of the laser amplifier system, step-index chalcogenide fiber, Pyro-camera, and FTIR-spectrometer.

In this Letter, we demonstrate a highly nonlinear mid-infrared supercontinuum source by launching fs-pulses into short pieces of step-index As_2S_3-fibers, generating a flat supercontinuum spanning the entire atmospheric mid-IR transmission window from 3 to 5 μm. This high-power and high repetition-rate mid-IR source can be used for spectroscopy as demonstrated in measurements with liquid carbon disulfide. The brilliance of the source is on the order of 10^{22} ph/s/mm^2/sr/0.1% BW. This is 4 orders of magnitude brighter than a typical synchrotron due to the single-mode beam output.

Figure 1 illustrates a schematic of the experimental setup. An NT&C 8 W Yb:KGW oscillator [16,17] with a pulse duration of 450 fs, a repetition rate of 42 MHz, and a central wavelength of 1.03 μm was used to pump a fiber-feedback optical parametric oscillator (OPO) [18,19]. The 300-fs signal pulses were further amplified with an optical parametric amplifier (OPA), delivering gap-free tunable idler pulses between 2.5 and 4.1 μm with an expected pulse duration of 300–450 fs and with an average output power of around 1 W (top part of Fig. 2). Both the OPO and the OPA employed a 10-mm-long PPLN crystal as nonlinear gain medium. A long-pass filter rejected the signal wave and transmitted the idler that was focused into the fiber via a 6-mm focal length IR aspherical lens. The As_2S_3-fiber had a step index design with a core diameters of 7 or 9 μm and a numerical aperture of 0.3 [20]. The resulting total transmission efficiency behind the outcoupling lens (4-mm focal length) was around 52%–64% depending on the wavelength. For pump wavelengths higher than 3.8 μm, the efficiency went down due to the impurity absorption losses in the fiber [20]. For the shorter pump wavelengths of the OPA, we observed deviations from a symmetrical Gaussian spatial beam profile that reduced the transmission efficiency as well. The coupling efficiency is mainly determined by a 5% loss at each IR objective and a Fresnel reflection loss of 15% at each fiber end face. The focal point was adjusted with the aid of an IR-camera (Pyrocam 3, Spiricon) to optimize the beam shape and to ensure single-mode operation in the effectively multi-moded fiber. The supercontinuum output was free-space-coupled to a Fourier transform infrared spectrometer (Frontier FTIR spectrometer, Perkin Elmer, range 1.2–30 μm).

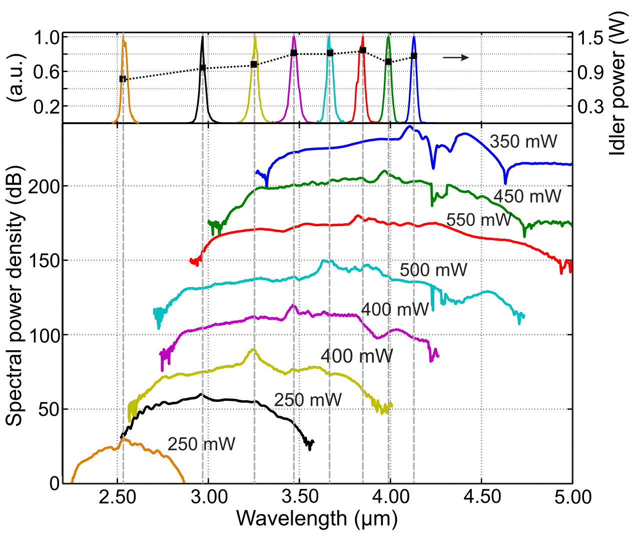

Fig. 2. Spectral broadening of the supercontinuum at maximum output power as a function of the launched idler wavelength for a fiber length of 13 cm and a core diameter of 9 μm. For better visibility, each spectrum is shifted upward by 30 dB. The average output power correspond to pulse energies between 6 and 13 nJ.

The spectral broadening was characterized in a 13-cm-long piece of 9 μm core diameter As_2S_3 chalcogenide fiber for different idler pump wavelengths as shown in Fig. 2. The eight pump wavelengths ranged between 2.53 and 4.13 μm, as displayed in the top part of Fig. 2. The generated supercontinuum spectra achieved an average output power between 250 and 550 mW (bottom part of Fig. 2), corresponding to pulse energies between 6 and 13 nJ without observing fiber damage. As the pump wavelength was increased, the spectral broadening could be enhanced up to a maximum bandwidth of 1.80 μm (at −20 dB points) at a launched idler wavelength of 3.83 μm. There, the spectrum spanned from 3.0 to 4.8 μm. The increase in the spectral broadening for longer pump wavelengths can be explained by approaching the ZDW and hence a reduction of normal dispersion. The estimated ZDW of the fundamental mode is calculated to be around 6.9 μm with normal dispersion of −18 ps/(nm km) at 3.8 μm [21]. For the two highest pump wavelengths around 4 μm, the spectral broadening could not be further enhanced due to the reduced transmission associated with higher losses in the fiber around the impurity band [9,20] and a lower available power of the OPA. The sometimes-observed dip at around 4.3 μm is due to atmospheric absorption mainly caused by CO_2. The measured beam profile of the output beam within the wide spectral range appeared to be near TEM_{00} at all pump wavelengths, but due to the lack of bandwidth filters, we were not able to determine this for certain in different narrow spectral ranges. However, at the shortest pump wavelength of 2.53 μm, we identified the excitation of a higher order mode, which still resulted in a spectral bandwidth larger than 550 nm. In the inset of Fig. 3, the beam profile is illustrated at a launched wavelength of 3.83 μm for the case of maximum output power. The cutoff wavelength for single-mode operation has been 3.56 μm [20]. However, also at smaller wavelengths mainly, the fundamental mode could be excited by proper alignment and adaptation of the focal spot diameter to the mode field diameter of the fundamental mode. By using a

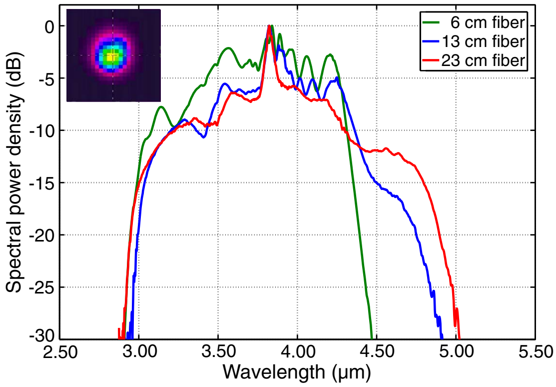

Fig. 3. Spectral broadening of the supercontinuum at maximum output power of 550 mW as a function of fiber length for a pump wavelength of 3.83 μm and a core diameter of 9 μm. (Inset) Mode profile for the 23-cm fiber at maximum output power of 550 mW.

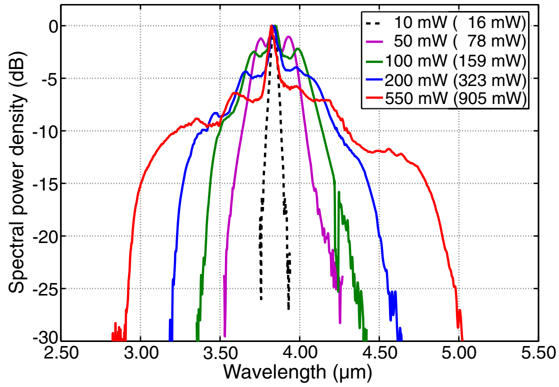

Fig. 4. Spectral evolution of the supercontinuum as a function of measured output power (input power) for a wavelength of 3.83 μm and a fiber length of 23 cm and a core diameter of 9 μm. SPM as broadening mechanism in the normal dispersion regime is visible as symmetric spectral evolution.

7-μm core diameter As_2S_3 chalcogenide fiber, mainly single-mode operation could also be achieved at a pump wavelength of 2.53 μm due to the reduced cutoff wavelength of 2.93 μm [20]. Owing to the smaller core size and better single-mode properties of the 7-μm fiber, the spectral broadening was enhanced at small pump wavelengths that shifted the small wavelength edge to 2.19 μm. However, the better performance at small pump wavelengths came at the cost of weaker spectral broadening at longer wavelength due to looser mode confinement and enhanced normal dispersion. The overall tuning range for the supercontinuum source with the 9-μm core diameter fiber extended from 2.27 μm up to 4.80 μm at the −20 dB points.

Figure 3 depicts the spectral broadening for different fiber lengths of 6, 13, and 23 cm at the most appropriate pump wavelength of 3.83 μm in case of the 9 μm core diameter fiber. The maximum achievable output power of 550 mW was the same for all three fiber lengths. By using longer fibers, the spectral broadening at the longer wavelength side could be further enhanced up to a wavelength of 4.9 μm. However, with increasing propagation length, simulations showed that the fs-pulses became more and more temporally broadened, and the amount of spectral broadening gradually diminished so that further enhancement of the fiber length will not push the longer wavelength edge substantially further in the infrared.

The evolution of the supercontinuum spectrum for a 23-cm-long fiber as a function of measured output power is displayed in Fig. 4 in the case of the 9 μm core diameter fiber. As the input power was increased, the spectrum broadened mostly symmetrically around the pump wavelength of 3.83 μm, whereas the longer wavelength components were slightly dominating. The process of supercontinuum generation with fs-pulses when pumping in the normal dispersion regime away from the ZDW was mainly driven by self-phase modulation (SPM) [22]. The approximately symmetric spectral properties were typical for the interaction of SPM and normal dispersion of the fiber. The supercontinuum bandwidth at an output power of 550 mW ranged from 2.95 to 4.90 μm. Overall, the step-index As_2S_3 chalcogenide fiber has been very robust and the spectral broadening remained repeatable over several weeks.

The robustness of the step-index design has allowed for higher transmission and higher average power in contrast to small core fiber designs such as suspended core or photonic crystal fibers. The specified transmission range of the fiber has ranged from 1.5 to 6.5 μm [20] and exceeded the maximum wavelength observed in the supercontinuum spectrum of Fig. 4. Increased pump power should enhance the bandwidth even further, while no damage or degradation of the fiber was observed for the applied powers. To demonstrate the stability and potential application of the supercontinuum source we performed measurements of the IR-transmission spectrum of liquid carbon disulfide around a wavelength of 3.5 μm (see Fig. 5). The white-light spectrum used to measure the transmission spectrum spanned from 3.1 to 3.8 μm with an average output power of 100 mW. Two consecutive measurements (each averaged over 20 scans) of an air-filled cuvette (Hellma Analytics QX 10 mm) showed an almost flat line at unity (red dashed curve). The IR-transmission spectrum of the CS_2-filled cuvette showed the characteristic twofold absorption peaks (red curve). For comparison reference data from NIST [23] are displayed in black in Fig. 5. The two ab-

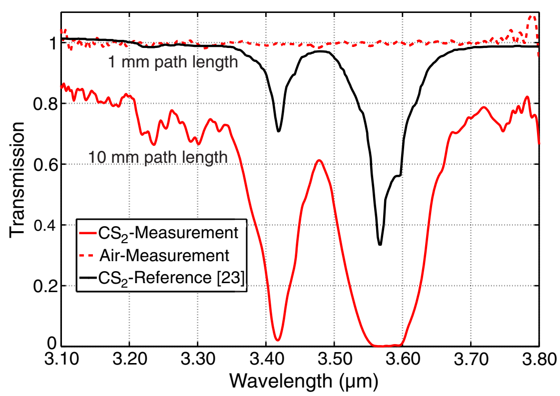

Fig. 5. IR-transmission spectrum of liquid carbon disulfide (CS_2) measured with the supercontinuum source at a pump wavelength of 3.47 μm and 100 mW output power. For comparison, we also plotted an air reference measurement and the reference data from NIST [23].

sorption peaks at 3.41 and 3.58 μm fit perfectly the literature values.

We presented a robust and stable white-light source with high average output power above 500 mW. The system was based on a recently developed post-amplified fiber-feedback OPO that delivered tunable fs-pulses at wavelengths from 2.5 to 4.1 μm. In a standard As_2S_3 step-index fiber, we achieved a total spectral bandwidth of 2.6 μm spanning from 2.3 to 4.9 μm. The variation of the spectral bandwidth was investigated by changing the pump wavelength, core diameter, fiber length, and pump power. When pumping a 23-cm-long 9-μm core diameter fiber at the appropriate wavelength of 3.8 μm, we obtained a supercontinuum that covered the important transparent atmospheric window between 3 and 5 μm. The broadband light source can be used in the field of mid-IR spectroscopy due the excellent mechanical properties of the step-index fiber design, its high brilliance, and its spectral flatness resulting from normal dispersion pumping. The stable operation was demonstrated by measurements of characteristic absorption bands of liquid CS_2.

Alexander von Humboldt Foundation; Baden-Württemberg Stiftung; Bundesministerium für Bildung und Forschung (BMBF); Deutsche Forschungsgemeinschaft (DFG); European Research Council (ERC, Complexplas); Zeiss-Stiftung.

The authors would like to thank G. Renz from DLR for the aid with the Pyrocamera.

REFERENCES

1. B. J. Eggleton, B. Luther-Davies, and K. Richardson, Nat. Photonics **5**, 141 (2011).
2. Y. Yu, X. Gai, T. Wang, P. Ma, R. Wang, Z. Yang, D.-Y. Choi, S. Madden, and B. Luther-Davies, Opt. Mater. Express **3**, 1075 (2013).
3. T. Wang, X. Gai, W. Wei, R. Wang, Z. Yang, X. Shen, S. Madden, and B. Luther-Davies, Opt. Mater. Express **4**, 1011 (2014).
4. O. Mouawad, J. Picot-Clémente, F. Amrani, C. Strutynski, J. Fatome, B. Kibler, F. Désévédavy, G. Gadret, J.-C. Jules, D. Deng, Y. Ohishi, and F. Smektala, Opt. Lett. **39**, 2684 (2014).
5. U. Møller, Y. Yu, I. Kubat, C. R. Petersen, X. Gai, L. Brilland, D. Méchin, C. Caillaud, J. Troles, B. Luther-Davies, and O. Bang, Opt. Express **23**, 3282 (2015).
6. W. Gao, Z. Duan, K. Asano, T. Cheng, D. Deng, M. Matsumoto, T. Misumi, T. Suzuki, and Y. Ohishi, Appl. Phys. B **116**, 847 (2014).
7. D. D. Hudson, M. Baudisch, D. Werdehausen, B. J. Eggleton, and J. Biegert, Opt. Lett. **39**, 5752 (2014).
8. C. R. Petersen, U. Møller, I. Kubat, B. Zhou, S. Dupont, J. Ramsay, T. Benson, S. Sujecki, N. Abdel-Moneim, Z. Tang, D. Furniss, A. Seddon, and O. Bang, Nat. Photonics **8**, 830 (2014).
9. R. R. Gattass, L. B. Shaw, V. Q. Nguyen, P. C. Pureza, I. D. Aggarwal, and J. S. Sanghera, Opt. Fiber Technol. **18**, 345 (2012).
10. S. Xie, F. Tani, J. C. Travers, P. Uebel, C. Caillaud, J. Troles, M. A. Schmidt, and P. St.J. Russell, Opt. Lett. **39**, 5216 (2014).
11. Y. Yu, X. Gai, P. Ma, D.-Y. Choi, Z. Yang, R. Wang, S. Debbarma, S. J. Madden, and B. Luther-Davies, Laser Photon. Rev. **8**, 792 (2014).
12. Y. Yu, B. Zhang, X. Gai, C. Zhai, S. Qi, W. Guo, Z. Yang, R. Wang, D.-Y. Choi, P. Ma, S. Madden, and B. Luther-Davies, Opt. Lett. **40**, 1081 (2015).
13. X. Jiang, N. Y. Joly, M. A. Finger, F. Babic, G. K. L. Wong, J. C. Travers, and P. St.J. Russell, Nat. Photonics **9**, 133 (2015).
14. W. Yang, B. Zhang, G. Xue, K. Yin, and J. Hou, Opt. Lett. **39**, 1849 (2014).
15. R. Thapa, D. Rhonehouse, D. Nguyen, K. Wiersma, C. Smith, J. Zong, and A. Chavez-Pirson, Proc. SPIE **8898**, 889808 (2013).
16. A. Steinmann, B. Metzger, R. Hegenbarth, and H. Giessen, in *Conference on Lasers and Electro-Optics*, OSA Technical Digest (CD) (Optical Society of America, 2011), paper CThAA5.
17. NT&C, Available at http://www.ntandc.de.
18. T. Südmeyer, J. Aus der Au, R. Paschotta, U. Keller, P. G. R. Smith, G. W. Ross, and D. C. Hanna, Opt. Lett. **26**, 304 (2001).
19. T. Steinle, F. Neubrech, A. Steinmann, X. Yin, and H. Giessen, Opt. Express **23**, 11105 (2015).
20. http://www.irflex.com/products/irf-s-series-chalcogenide-nonlinear-mid-infrared-fiber.
21. W. S. Rodney, I. H. Malitson, and T. A. King, J. Opt. Soc. Am. **48**, 633 (1958).
22. J. M. Dudley, G. Genty, and S. Coen, Rev. Mod. Phys. **78**, 1135 (2006).
23. http://webbook.nist.gov/cgi/cbook.cgi?ID=C75150&Type=IR-SPEC&Index=3#IR-SPEC.